Article

Clay Minerals and Sr-Nd Isotope Compositions of Core CG 1601 in the Northwest Pacific: Implications for Material Source and Rare Earth Elements Enrichments

Zhongrong Qiu [1,2,3], Weilin Ma [2,3,*], Chunhui Tao [1,2,3,*], Andrea Koschinsky [4] and Siyi Hu [2,3]

1 Ocean College, Zhejiang University, Zhoushan 316000, China; qzr@zju.edu.cn
2 Key Laboratory of Submarine Geosciences, Ministry of Natural Resources, Hangzhou 310012, China; niudun2901@163.com
3 Second Institute of Oceanography, Ministry of Natural Resources, Hangzhou 310012, China
4 Department of Physics and Earth Sciences, Jacobs University Bremen, 28759 Bremen, Germany; a.koschinsky@jacobs-university.de
* Correspondence: maweilin308@sina.com (W.M.); taochunhuimail@163.com (C.T.)

Abstract: Deep-sea sediments generally refer to the sediments distributed on the seafloor with a depth of more than 2000 m. Many rare earth elements and yttrium (REY)-rich sediments were recently discovered in the sea area of Minamitorishima Island, Northwest Pacific. To understand the material source and REY enrichments of sediments in this area, here, we performed clay minerals and Sr-Nd isotopes analyses on gravity core GC1601 gained in the Southeast Sea area of Minamitorishima Island. The clay mineral composition of the core is very similar to that of terrigenous materials, and its montmorillonite/illite (M/I) ratio ranges from 0.09 to 0.20 with an average of 0.15, indicating that the sediments in the study area should be mainly dominated by terrestrial sources, consistent with the results of Sr-Nd isotope study. Considering that the study area is far away from the mainland and in the downwind direction of the East Asian monsoon, we propose that the terrigenous material of the sediments in the study area is likely East Asian dust. The εNd values of GC1601 show a positive correlation with P_2O_5, Co, Ni, and Cu, and have an increasing trend with increasing depth, approaching that of the seawater, indicating that the sedimentary environment in the area is relatively stable. Although the total REY content (ΣREY) of the core increases with depth, due to the large supply of terrigenous materials for the sediments, it is difficult for the study area to form high-grade REY-rich muds.

Keywords: Northwest Pacific; deep-sea sediments; material source; sedimentary environment; REY enrichments

1. Introduction

Deep-sea sediments generally refer to the sediments distributed on the seafloor with a depth of >2000 m, which contains clay minerals, biological residues (phosphorus fish bone fragments and a small amount of calcium and siliceous biological fragments), phillipsite, micro-nodules, barite, and a small amount of detrital minerals such as quartz and feldspar [1,2].

The Northwest Pacific seamounts are located east of the Philippine Basin and the Mariana Trench, an area in transition from the back-arc basin to the ocean basin. Many cobalt-rich crusts and polymetallic nodules have been formed in this area, making it one of the most promising areas for metal bound to iron manganese oxides [3–5]. In addition, recent studies on deep-sea sediments showed that this area contains lots of rare earth elements and yttrium (REY) rich sediments, which has become one of the most promising REY-rich metallogenic areas [6].

The formation of marine metal resources is closely related to its environment and source of ore-forming materials. Most research in this area focuses on mineral resource

properties and potentials, while little attention has been paid to the metallogenic environment and provenance. For example, Fujinaga et al. [7] studied a large number of sediment cores in the Exclusive Economic Zone (EEZ) of Minamitorishima Island and found that sediments in the southern part of the EEZ are enriched in REY (>1000 ppm), while the total REY content (ΣREY) of sediments in the northern area is relatively low, (<400 ppm), which may be affected by the dilution of terrigenous materials. However, there is little discussion on the causes of REY depletion in sediments and how they are affected by terrigenous materials in this area.

The polymetallic nodules study area of the China Ocean DY-40B cruise is adjacent to the EEZ of Minamitorishima Island and also located in the Marcus-Wake Seamount area. The topography and geomorphology of the study area are similar to that of the EEZ of Minamitorishima Island. However, the average REY content in surface sediments is only about 350 ppm, which is much lower than that of EEZ of Minamitorishima Island (deep-sea mud containing 5000 ppm total REY content was discovered in this area) [8–10]. Are such low-grade REY contents directly related to the material source? If so, what kind of material source is it dominated by? The seamounts in Northwest Pacific are located downwind of the East Asian monsoon and may receive material supplies from land-based sources, although they are far from the mainland. Therefore, an in-depth study of the composition and characteristics of the sediments in the basin and a systematic analysis of their material sources and source structure attributes are of great scientific significance for revealing the sedimentary evolution of the area, deepening the understanding of seabed metal mineralization of polymetallic nodules, cobalt-rich crusts, and REY-rich sediments and guiding resource exploration.

2. Regional Setting

The Northwest Pacific Seamounts are located in the northwestern Pacific Ocean, southeast of the Japanese Islands, west of the Hawaiian Islands, and east of the Mariana Trench (Figure 1). Several seamount chains are developed within the zone, such as the Marcus-Wake Seamounts, Ogasawara Ridge, Magellan Seamounts, Gilbert Ridge, Central Pacific Seamounts, and Marshall Seamounts. The gravity core (No. GC1601) used in this study was recovered from the Marcus-Wake Seamounts area (Figure 1). The seamounts of the Northwest Pacific Ocean are enriched in lots of mineral resources such as cobalt-rich crusts and seabed phosphorite and are currently considered to be the most promising cobalt-rich crust mineralization areas on the seafloor [11–15].
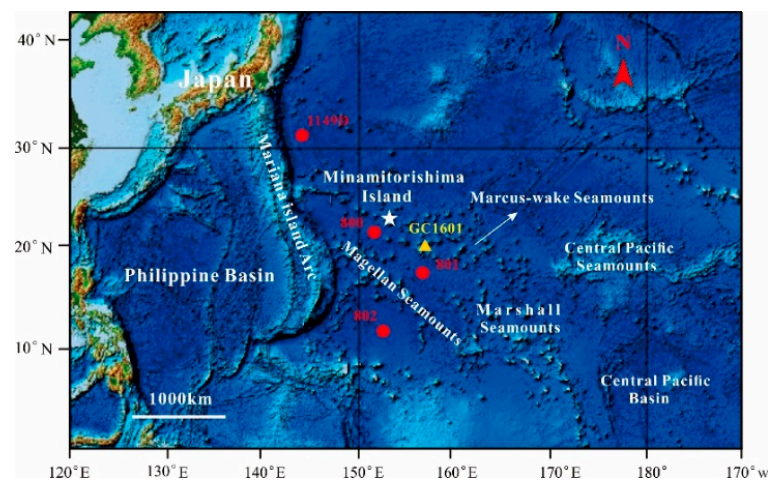

Figure 1. Geography and location of GC1601 from Northwest Pacific. The red dots represent the geographic locations of Ocean Drilling Program (ODP) sites.

The volcanoes in the zone were mainly formed in the Early to Middle Cretaceous, and the volcanic basement is Jurassic tholeiite and alkaline basalt. The sedimentary strata

above the basement include Middle Jurassic to Late Cretaceous radiolarians, mudstone, flint, volcanic clastic turbidites, kaolin porcelain rocks, and Cenozoic deep-sea clay and calcareous soft mud [16]. Due to the lack of terrigenous clastic input, the sediments on the surface of oceanic crust in the seamount area are very thin, mostly <500 m (e.g., ODP sites 801 and 1149) [17,18]. Generally, sediment thickness in the ocean basin is greater than that in the vicinity of the seamounts, and the region with the greatest sediment thickness is in the Eastern Mariana Basin in the Southeastern part of the Magellan Seamounts, where the sediment thickness >1000 m. Pelagic clay, bioclastic, and volcanic ash are the main components of the sediments [2,19].

3. Sample and Methods

The gravity core GC1601(location, 157.21, 21.31° N; total length = 250 cm; water depth = 5336 m) was retrieved from the Southeast Sea area of Minamitorishima Island. The texture of the sample is uniform and yellowish-brown (Figure 2).
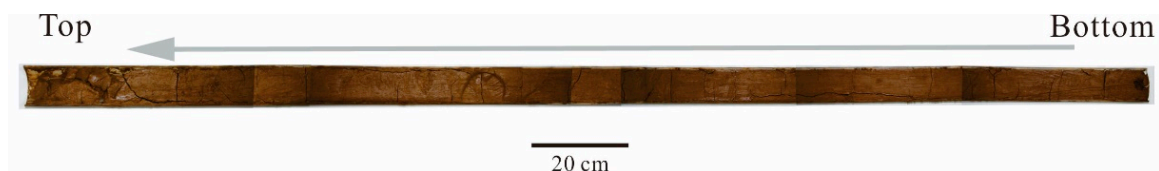

Figure 2. Appearance characteristics of GC1601.

3.1. Clay Minerals

The clay samples were analyzed by extracting <2 μm components of the sediment, removing organic matter with 30% H_2O_2, removing $CaCO_3$ with dilute 10% HCl, removing the components of <2 μm, and using the smear method to make natural air-dried clay-oriented sheets for X-ray diffraction analysis (XRD), and the remaining part was dried at 50 °C for other analysis. The qualitative analysis of clay minerals was mainly carried out by ethylene glycol vapor saturation on the same clay-oriented flakes and then tested separately by XRD. The identification of each clay mineral is mainly based on the characteristics of its (001) diffraction peak. The instrument type and test conditions used for the analysis were: a Dutch X'Pert PRO X-ray diffractometer from the Second Institute of Oceanography, Ministry of Natural Resources, with an operating voltage of 45 kV, an operating current of 40 mA, a natural slice scan range of 3°~35° (2θ), and scanning speed of 1.8°/min. All analytical tests of the same batch of samples were carried out under the same conditions mentioned above. The measured diffraction data and plots were processed using MDI Jade 6 software.

The relevant contents of clay minerals were calculated according to the modified method of Biscaye [20]. That is, the peak areas of three sets of characteristic peaks of four minerals, montmorillonite (17 Å), illite (10 Å), chlorite (7 Å) + kaolinite (7 Å), on the glycol saturation sheet diffraction peaks were used as the base data, and the peak areas of the corresponding characteristic peaks of each clay mineral were multiplied by their respective weighting factors. The weight factor of montmorillonite was determined as 1, illite as 4, and chlorite + kaolinite as 2. The relative content of chlorite to kaolinite was calculated as the ratio of peak heights around 3.5 Å at about 25 °C (2θ).

Following are the calculation formula:

$$B = B_1 + 4B_2 + 2B_3$$

$$C_1 = B_1/B \times 100\%$$

$$C_2 = 4B_2/B \times 100\%$$ (1)

$$C_3 = 2B_3/B \times 1/(L+1) \times 100\%$$

$$C_4 = 2B_3/B \times L/(L+1) \times 100\%$$

where B is the total area, B_1 is the area of the montmorillonite peak (17 Å), B_2 is the area of illite peak (10 Å), B_3 is the chlorite + kaolinite peak (7 Å) area. C_1 is the percent montmorillonite mineral content (%), C_2 is the percent of illite mineral content (%), L is the ratio of kaolinite peak to chlorite peak height (3.5 Å), C_3 is the percent of chlorite mineral content (%), and C_4 is the percent of kaolinite minerals (%).

3.2. Sr-Nd Isotopes

Sr-Nd isotope analysis of bulk sediments in this study was carried out by multireceiver type inductively coupled plasma mass spectrometry (MC-ICP-MS) (Thermo Fisher Scientific Neptune Plus), and the main analytical procedure was as follows.

The sample was accurately weighed to 0.25 g and placed in a Teflon cuvette, 0.5 mL HNO_3 (16 mol/L) and 1.5 mL HF (32 mol/L) were added, the sample was digested by closed heating at 190 °C for 48 h. HF was evaporated at 160 °C, 3 mL 1:1 HNO_3 was added, and the sample was redissolved at 150 °C for 6 h. The weight of the solution was set to 25 g. For Sr, the appropriate amount of sample solution was centrifuged, and the supernatant was taken. The sample solution containing Sr was obtained by evaporating, adjusting the acidity, and purifying Sr using Sr-specific resin separately. Nd was collected as needed, the sample solution was centrifuged, the supernatant was evaporated, the acidity was adjusted, and Nd was separated and purified using Lanthanide potent resin to obtain an Nd-containing sample solution. The $^{87}Sr/^{86}Sr$ and $^{143}Nd/^{144}Nd$ values were determined using a Thermo Fisher Scientific multireceiver inductively coupled plasma mass spectrometer Neptune Plus MC-ICP-MS. The $^{86}Sr/^{88}Sr$ value (0.1194) and $^{146}Nd/^{144}Nd$ value (0.7219) are used for isotope fractionation correction according to the natural abundance of stable isotope ratio. (the uncertainty in the $^{87}Sr/^{86}Sr$ and $^{143}Nd/^{144}Nd$ ratios are 2σ and the number of measurements, n = 160). Sr and Nd solution/reference material were used NBS987 for Sr and Thermo Fisher Tune for Nd. The long-term average $^{87}Sr/^{86}Sr$ ratio measured by NBS987 is 0.71028 ± 0.00002, and it is 0.51238 ± 0.00002 for $^{143}Nd/^{144}Nd$ ratios, which are consistent with the recommended values. Geochemical reference materials of USGS BCR-2, BHVO-2, AVG-2, and RGM-2 were used as quality control. The results of Sr-Nd isotope ratios of the samples in this study were within the error range and consistent with the values reported by Chen et al. [21]. The measurements were performed at the Nanjing Hongchuang Geological Survey Technology Limited-Service Company.

4. Results

4.1. Clay Minerals

The percentages of the four main clay minerals (montmorillonite, illite, chlorite, and kaolinite) of GC1601 gravity core are shown in Table 1, where illite has the highest fractions (62%~67%) with an average value of 64% among these four main clay minerals, followed by chlorite (5.7%–18.8%) with an average value of 17.4%. The fractions of montmorillonite and kaolinite are relatively low, ranging from 5.8% to 12.6%, 8.4% to 9.5%, and with an average of 9.5% and 8.9%, respectively. In this study, the illite chemical index (CI) was calculated from the ratio of peak areas at 5 Å and 10 Å from the XRD diffraction curves of glycol slices and the half-peak width (Full Wave at Half Maximum-FWHM) at 10 Å was also used to indicate the crystallinity of illite. The range of illite CI is from 0.36 to 0.46 with the mean value of 0.42, and the range of illite crystallinity was 0.26°Δ 2θ~0.29°Δ 2θ with the mean value of 0.28°Δ 2θ. The montmorillonite/illite (M/I) ratios range from 0.09 to 0.20 and with a mean value of 0.15. The combination pattern of clay minerals of our sediment sample is the illite-chlorite-montmorillonite-kaolinite type.

The relative contents of the four major clay minerals and the vertical variations of the related parameters in the GC1601 are shown in Figure 3. Illite and montmorillonite profiles show opposite trends and nearly mirror image characteristics, suggesting they are derived from different sources. Kaolinite and chlorite profiles show slightly similar trends, indicating that they may have the same material origin. Profile distribution of the four clay

minerals does not show any obvious abrupt change, which may indicate relatively stable clay source materials in the study area during deposition.

Table 1. Clay minerals compositions of GC1601.

| Layer/cm | Relative Content of Clay Minerals (%) | | | | M/I | Illite | |
	Montmorillonite	Illite	Kaolinite	Chlorite		CI	Crystallinity
0–10	9.0	63	9.5	18.8	0.14	0.39	0.29
10–20	8.9	64	9.0	17.7	0.14	0.36	0.28
20–30	8.7	64	8.8	18.2	0.13	0.40	0.28
30–40	8.9	64	9.1	18.0	0.14	0.42	0.29
40–50	10.1	63	8.8	18.3	0.16	0.45	0.28
50–60	10.1	64	8.7	17.6	0.16	0.39	0.28
60–70	10.0	64	8.6	17.7	0.16	0.42	0.28
70–80	9.8	63	9.0	17.9	0.15	0.41	0.27
80–90	10.1	63	9.1	17.6	0.16	0.42	0.28
90–100	11.2	63	8.5	17.2	0.18	0.40	0.28
100–110	11.7	62	8.9	17.2	0.19	0.42	0.27
110–120	12.4	63	8.8	16.0	0.20	0.42	0.29
120–130	9.8	64	8.7	17.2	0.15	0.42	0.28
130–140	6.8	67	9.0	17.1	0.10	0.43	0.29
140–150	10.7	63	8.8	17.1	0.17	0.40	0.27
150–160	9.7	65	8.6	17.0	0.15	0.43	0.28
160–170	5.8	66	9.2	18.7	0.09	0.44	0.27
170–180	11.4	64	8.4	16.5	0.18	0.41	0.28
180–190	6.5	67	9.1	17.6	0.10	0.46	0.28
190–200	6.9	66	9.0	17.9	0.10	0.41	0.27
200–210	8.8	65	9.0	16.9	0.13	0.42	0.28
210–220	12.6	63	8.6	15.7	0.20	0.41	0.28
220–230	9.0	65	9.1	17.3	0.14	0.42	0.27
230–240	9.6	64	8.4	18.0	0.15	0.44	0.26
240–250	9.9	65	8.8	16.4	0.15	0.45	0.28
Max	12.6	67	9.5	18.8	0.20	0.46	0.29
Min	5.8	62	8.4	15.7	0.09	0.36	0.26
Average	9.5	64	8.9	17.4	0.15	0.42	0.28

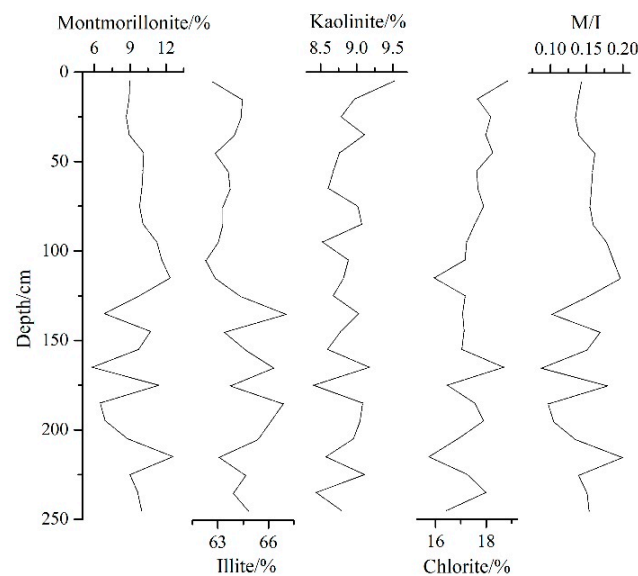Note: M/I represents montmorillonite/illite, and CI represents chemical index.

Figure 3. Profile distribution of clay minerals and M/I ratios from GC1601.

4.2. Sr-Nd Isotopes

The ^{87}Sr/^{86}Sr and ^{143}Nd/^{144}Nd ratios of the nine samples of GC1601 core are shown in Table 2. The ^{87}Sr/^{86}Sr values of the GC1601 core sample is 0.714828~0.715949, with an average value of 0.715227, and overall, the variation range of ^{87}Sr/^{86}Sr values is small. The ^{143}Nd/^{144}Nd values were 0.512223~0.512297 with a mean value of 0.512269. Similar to ^{87}Sr/^{86}Sr, the ^{143}Nd/^{144}Nd variation range was also small. Similarly, the εNd(0) values varied from −6.65 to −8.10 with a mean value of −7.20, and its variation range was also relatively small. Small variation ranges and good homogeneity of ^{87}Sr/^{86}Sr, ^{143}Nd/^{144}Nd, and εNd(0) values indicate that the material sources in the study area are relatively stable over time.

Table 2. Sr-Nd isotope values of GC1601.

No	Layer/cm	^{87}Sr/^{86}Sr	$2\sigma/\times 10^{-6}$	^{147}Sm/^{144}Nd	^{143}Nd/^{144}Nd	$2\sigma/\times 10^{-6}$	εNd(0)
N1	0–10	0.714976	4	0.131819	0.512223	6	−8.10
N2	30–40	0.715124	5	0.125666	0.512278	6	−7.02
N3	60–70	0.715230	4	0.122499	0.512283	7	−6.92
N4	90–100	0.715180	4	0.127205	0.512274	5	−7.10
N5	120–130	0.715281	4	0.128368	0.512250	7	−7.57
N6	150–160	0.715949	4	0.123743	0.512255	7	−7.47
N7	180–190	0.715415	4	0.120971	0.512271	9	−7.16
N8	210–220	0.715062	4	0.128217	0.512288	6	−6.83
N9	240–250	0.714828	4	0.130350	0.512297	7	−6.65
	Average	0.715227	4	0.126538	0.512269	7	−7.20
	Max	0.715949	5	0.131819	0.512297	9	−6.65
	Min	0.714828	4	0.120971	0.512223	5	−8.10

Note: εNd(0) = [(^{143}Nd/^{144}Nd)$_{sample}$/(^{143}Nd/^{144}Nd)$_{CHUR}$ − 1] × 10000, (^{143}Nd/^{144}Nd)$_{CHUR}$ = 0.512638.

5. Discussion

5.1. Material Sources

5.1.1. Clay Mineral Indication

The most common clay minerals in marine sediments are montmorillonite, illite, kaolinite, and chlorite. They are extremely fine-grained and distributed in almost all regions of the seafloor [22,23]. The composition and distribution patterns of clay minerals record information of transports, redepositions, and environmental evolutions and are very important indicators for the study of marine sedimentation, marine sediment characteristics, palaeoceanographic environment, and sediments source [24–26].

As one of the clay minerals, montmorillonite is widely distributed in the ocean, and its genesis is relatively complex [27]. At present, there are two main sources of montmorillonite in the ocean: terrestrial detritus and submarine volcanic material. The first type of montmorillonite from terrestrial clasts is formed by hydrolysis of parent rocks from surrounding continents under warm to semiarid climatic conditions and is transported from rivers to the ocean. The second type of montmorillonite from submarine volcanic material is mainly associated with volcanic activity, hydrothermal alteration of volcanic material, weathering, and hydrolysis [28,29]. Previous studies suggested that when the sedimentary material source is mainly supplied by terrestrial material, the content of montmorillonite is relatively low, generally not exceeding 20% [30]. When montmorillonite is mainly derived from volcanic material alteration, the content of montmorillonite usually increases with the increase of volcanic material input in the sediment, and its content can even reach more than 50% [31]. The high percentage of montmorillonite generally indicates high volcanic hydrothermal activities [32,33]. The average content of montmorillonite in the sediments of this study is only 9.5% (Table 1), implying that the sediment material source in the area is mainly of terrestrial origin.

Illite is one of the most common clay minerals in marine sediments, is basically considered to be of terrestrial origin, and is mainly imported into the ocean through rivers

and wind [34]. The relative content of illite is 64% (Table 1), which is similar to illite compositions in the clays of terrestrial origin such as Yellow River and Yangtze River sediment [35], implying that illite in this study should also be of terrestrial origin. In addition, the chemical index (CI) of illite in this study ranges from 0.36 to 0.46, with a mean value of 0.42. The illite crystallinity varies from $0.26°\Delta\,2\theta$ to $0.29°\Delta\,2\theta$, with a mean value of $0.28°\Delta\,2\theta$ (Table 1), which are very close to the CI and crystallinity of illite of Chinese loess (the CI and crystallinity of illite of Chinese loess are 0.4 and $0.33°\Delta\,2\theta$, respectively) [30]. Small values of illite crystallinity indicate a better crystallization and refer to dry and cold climatic conditions, while when illite CI is below 0.5, it usually indicates physical weathering. Considering that the study area is far from the continent and riverine input is impossible, we speculate that the high content of illite in the study area mainly refers to eolian dust input from the Asian continent.

The relative contents of illite, montmorillonite, kaolinite, and chlorite can be used as terminal elements for triangle projection analysis (Figure 4). The Mariana Trough and the Philippine Trench are strongly influenced by volcanic hydrothermalism, and the sediments in these areas usually have a large amount of volcanic material input [36]. Taking sediments of these areas as the volcanic end member, we found that clay mineral assemblages in these two regions are different from those of this study, which are similar to the Chinese loess and Yangtze River sediments, etc., indicating terrestrial sources. Considering the North American Shale-normalized REE distribution pattern of the study sample is similar to that of Chinese Loess [9], it indicates that the material supply of volcanic hydrothermal materials to the study area is very limited.
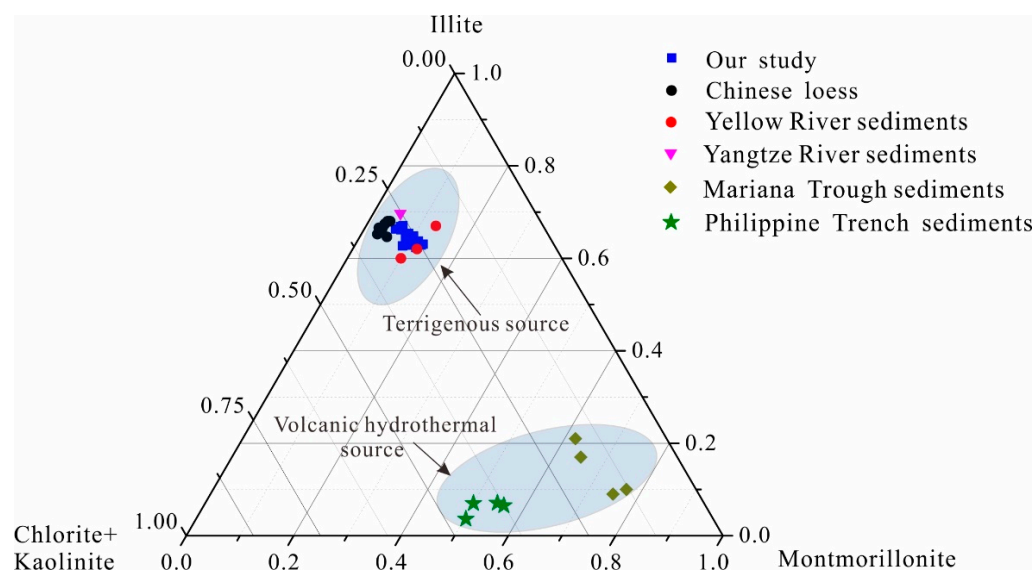

Figure 4. Ternary showing variation in clay mineral compositions of sediments for GC1601 and other geological regions. Chinese loess data are from [37], Yellow River sediments data are from [38–40], Yangtze River sediments data are from [41], Mariana Trough sediments data are from [42], Philippine Trench sediments data are from [43,44].

Previous studies also take M/I values as a proxy for eolian dust input [23,30], with a low M/I ratio indicating a high proportion of terrigenous clay minerals and a low proportion of clay minerals altered by volcanic material and hydrothermal fluid. When the M/I ratio becomes larger, it indicates higher content of clay minerals altered by volcanic material and hydrothermal fluid and low content of terrigenous clay minerals [8,45]. A previous study suggested that all clays in the Atlantic are of terrestrial origin [34], M/I ratios of sediments from the North and South Atlantic are 0.29 and 0.55, respectively. By contrast, M/I ratios of the core are quite low, with a mean value of 0.15, which is significantly lower than that of Atlantic sediments, suggesting that clay minerals in the study area are

dominated by terrestrial sources. In addition, smear identification also shows that the clay fractions account for more than 90% of the visual field [2], which further implies that the sediments in the study area should be mainly dominated by terrestrial sources.

5.1.2. Sr-Nd Isotope Indications

Similar to REY, the Sr-Nd isotopic composition in marine sediments are mainly controlled by the parent rocks, and the isotopic composition of which will hardly be affected by late weathering, denudation, transported redeposits, hydrodynamics, etc. Thus, Sr-Nd isotopes can reflect the nature of sediment sources and serve as an important tool for sediment sources studies [46–48]. The Sr-Nd isotope ratios of core GC1601 and other geological bodies are shown in Figure 5, in which we can see Chinese loess, Yangtze River sediments, and North Central Pacific silicates sediments are mainly terrestrial sources, while Mariana Trough Basalts (MTB) and Mid-Ocean Ridge Basalts (MORB) represent the source endmember of the volcanic hydrothermal source. All the sediment samples of core GC1601 fall into the terrestrial source field, which further indicates that the sediment composition of the study area is mainly dominated by terrestrial sources. The MORB and MTB, which represent the volcanic hydrothermal component, have high εNd values (mean values > 7) and low $^{87}Sr/^{86}Sr$ ratios, which are significantly different from that of GC1601 (Figure 5). This indicates that the contribution of volcanic hydrothermal components to the study area is very limited, which is consistent with previous studies [2].
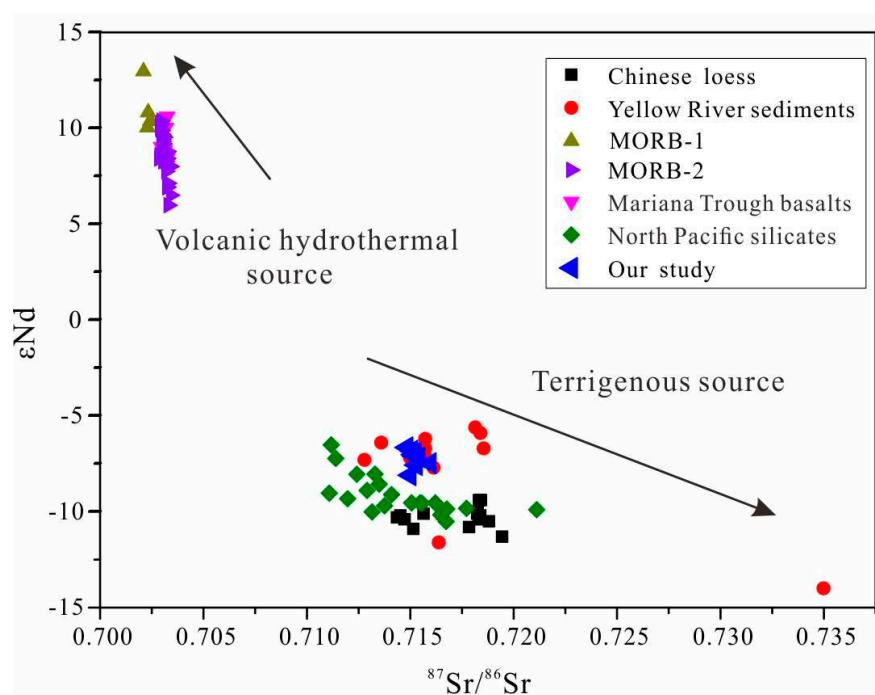

Figure 5. Sr-Nd isotopic compositions of GC1601 and other geological materials. Chinese loess data are from [49]; Yangtze River sediments data are from [50,51]; MORB-1 data are from [52]; MORB-2 data are from [53] Mariana Trough basalts data are from [54]; North Pacific silicates data are from [55].

In addition, previous studies have suggested that East Asian dust can transport for a long-distance and large-scale, and its transportation extends eastward from China [56] to Korea and Japan [57,58], and even to the North Pacific and western North America [55]. The GC1601 core was recovered from the Marcus-Wake Seamounts, Northwest Pacific Ocean, about 2500 km from mainland Japan, which will affect the material input of the East Asian dust and westerly geographically (Figure 6). Considering that the study area is far away from the mainland and rivers, it is inferred that the terrestrial source of the sediments in the study area is likely to be East Asian dust.
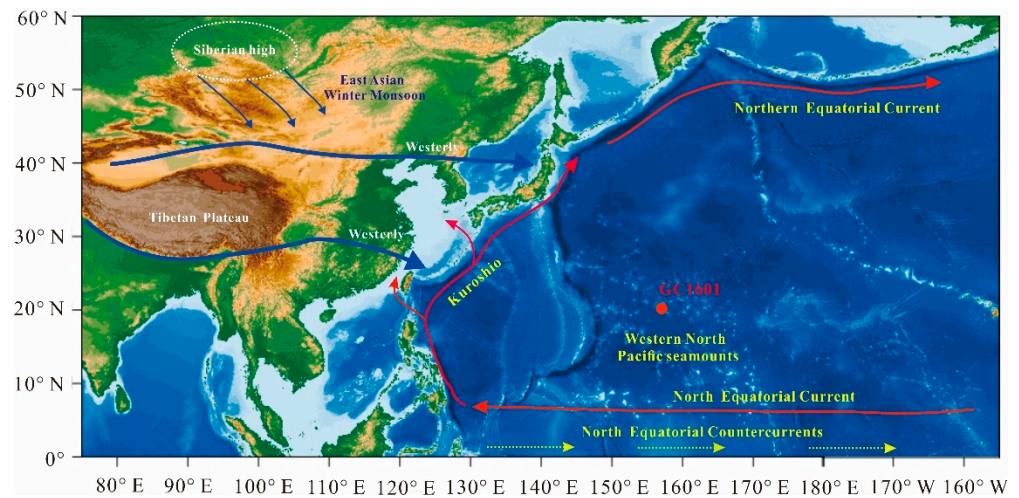
Figure 6. Monsoon and Ocean current in the western Pacific (Modified after [59,60]).

5.2. Sedimentary Environment

The εNd(0) values of samples in this study showed an overall increase with depth (Figure 7). Wang et al. [61] studied the REY-rich sediments in the Central and Western Pacific Ocean and found that their εNd values were close to that of seawater, suggesting that the REY in REY-rich sediments maybe have derived directly from seawater. The samples in this study were collected at a water depth of 5336 m, which is below the carbonate compensation depth (CCD), and the smear identification also suggested that biogenic carbonate was completely dissolved while the siliceous biomass content was also very low [2]. Comparing the εNd(0) values of seawater from the same region (Northwest Pacific) at an approximate depth (5060 m) with that of this study [62], we find that the εNd(0) values of GC1601 are generally close to that of seawater (εNd(0) = −5.09 ± 0.52 [62]) with increasing depth, which indicates that core GC1601 was gradually influenced by seawater with increasing sedimentary depth (Figure 7). Such "seawater effect" can be interpreted as some autobiomass-like siliceous organisms (e.g., radiolarian fragments and diatoms), biogenic phosphates, etc., from the ocean codeposited into the sediments.
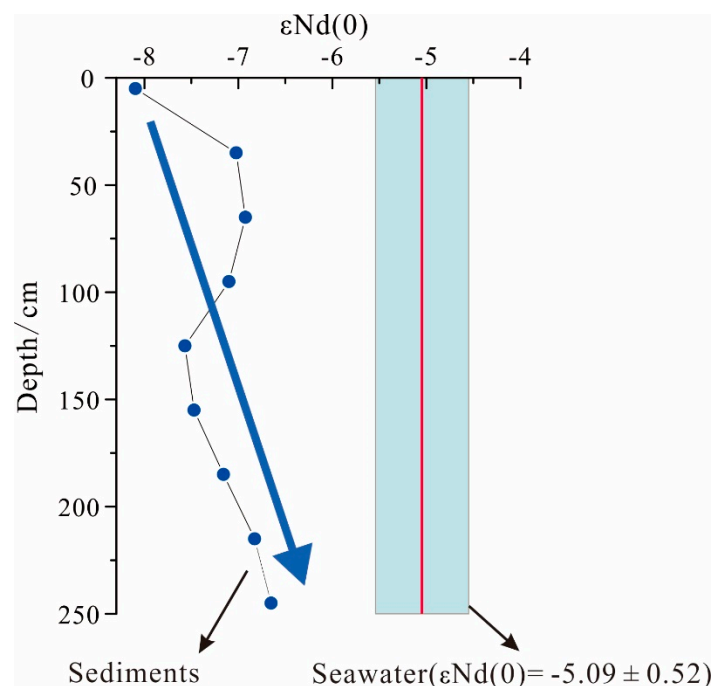

Figure 7. Profile distribution of εNd(0) in GC1601 and seawater.

P_2O_5 of deep-sea sediments is generally considered to represent biogenic phosphates [63], while Co, Ni, and Cu are typical hydrogenic components [2]. P_2O_5, Cu, Ni, Co contents, and $\varepsilon Nd(0)$ value in GC1601 core all show an obvious positive correlation (Figure 8). The authigenic and hydrogenic components such as P_2O_5, Co, Ni, and Cu increase gradually with increasing depth in the sediment profile, indicating that the depositional environment of the deposition area is relatively stable, which further suggests the sediments of the study area are not influenced by currents such as the North Equatorial Current and Kuroshio during the slow deposition process. At the same time, combining the positive correlation between $\varepsilon Nd(0)$ and P_2O_5, Co, Ni, and Cu (Figure 8a,c,d), and the interesting result that $\varepsilon Nd(0)$ values of CG1601 are close to that of seawater at greater depth, it is suggested that sediments of the study area steadily received the slow modification by seawater during the early diagenetic stage. Such slow modification of seawater provides sufficient time for the marine authigenic biomass to enter the sediments under a relatively stable sedimentary environment.
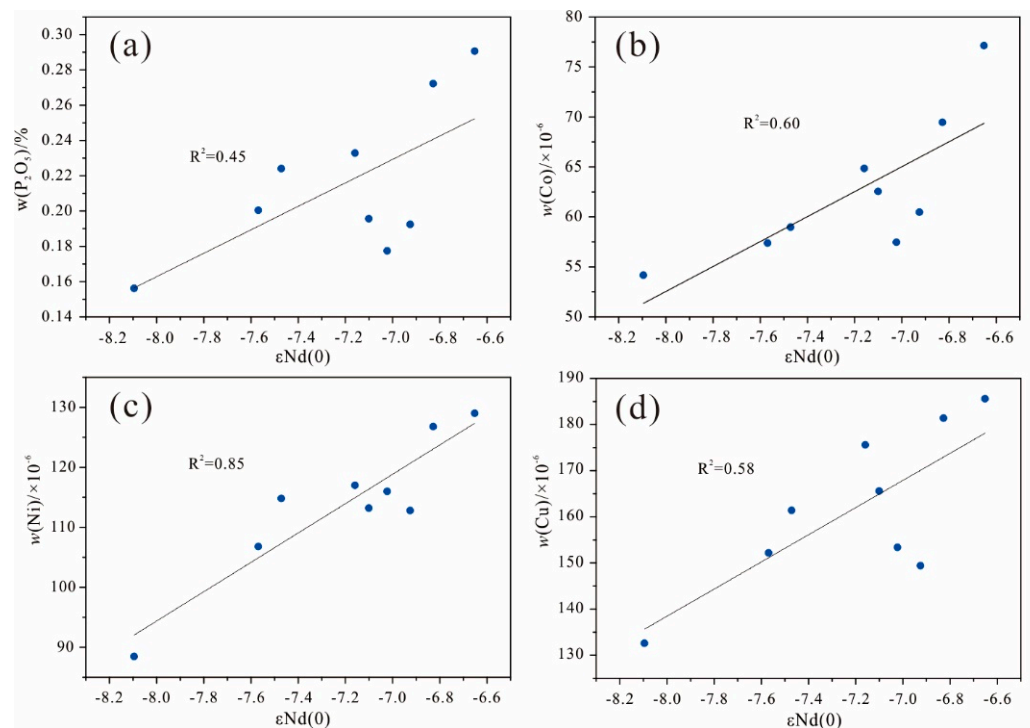

Figure 8. Correlation between $\varepsilon Nd(0)$ and P_2O_5 (**a**), Co (**b**), Ni (**c**), Cu (**d**) in CG1601. Note that concentrations of major and trace elements were measured per 2cm while $\varepsilon Nd(0)$ was measured per 10 cm, in order to compare with $\varepsilon Nd(0)$ of the same depths, 5 points average of those concentrations (major and trace elements) were calculated with 10 cm interval through the core.

5.3. Indication of the REY Enrichments

Many surface sediment samples were taken from the Sea area of Minamitorishima Island, and it was found that sediments in the southern Sea area of Minamitorishima Island exhibit a high ΣREY, above 400 ppm, and some sediments even had a ΣREY of nearly 7000 ppm (e.g., KR13-02 PC05) [64]. By contrast, the ΣREY of a series of sediments stations taken from the northern sea area of Minamitorishima Island was very low, almost all <400 ppm [7]. Fujinaga et al. [7] suggested that the dilution by terrigenous materials (possibly eolian dust) is the main cause of the REY-poor sediments in the North Sea area of Minamitorishima Island. CG1601 core was collected from the South Sea area of Minamitorishima Island, very close to the Japanese EEZ, and the REY contents of the core were all very low, generally between 200 ppm and 350 ppm, which is similar to that of sediments from the northern Sea area of Minamitorishima Island. Therefore, it

can be concluded that the reason for the poor REY in the East and the North Sea area of Minamitorishima Island should be the same, i.e., strong dilution by Asian dust materials.

However, the South Sea area of Minamitorishima Island is very similar to the East and the North Sea area of Minamitorishima Island in terms of sedimentary water depth and tectonic environment, thus if the sediments in the North and East Sea area of Minamitorishima Island are affected by terrigenous materials, then the sediments with nearly the same types in the South Sea area of Minamitorishima Island, which are very close to each other in relation to tectonic environments, should also be "affected". However, the sediments in the South Sea area of Minamitorishima Island are highly enriched in ΣREY and do not seem to be diluted by terrigenous materials. Previous studies have indicated that the formation of REY-rich muds likely occurred in pelagic realms with very low sedimentation rates [65,66]. When the sedimentation rates are very low, dissolved metals (e.g., Co, Ni, Cu, and REY) or certain colloidal particles (e.g., Fe/Mn oxyhydroxides) in seawater can be slowly deposited on the seafloor without significant dilution by terrigenous detrital components or calcareous/siliceous microsomal fossils, which not only leads to the efficient adsorption of these elements by their carrier minerals (biophosphates or Mn-oxides), but also to the significant accumulation of these carrier minerals in the sediments [66,67]. The Lower Circumpolar Deep Water (LCDW) flow through the Northwest Pacific seamount (Figure 9), which has a depth distribution of 4000–5000 m [59], is very close to the sediment's bathymetry in the region [10]. Yasukawa et al. [59] suggested that it was the influence of LCDW that led to a significantly low sedimentation rate in the South Sea area of Minamitorishima Island, which resulted in the accumulation of large amounts of biogenic phosphate fractions in sediments and ultimately in high enrichment of ΣREY.
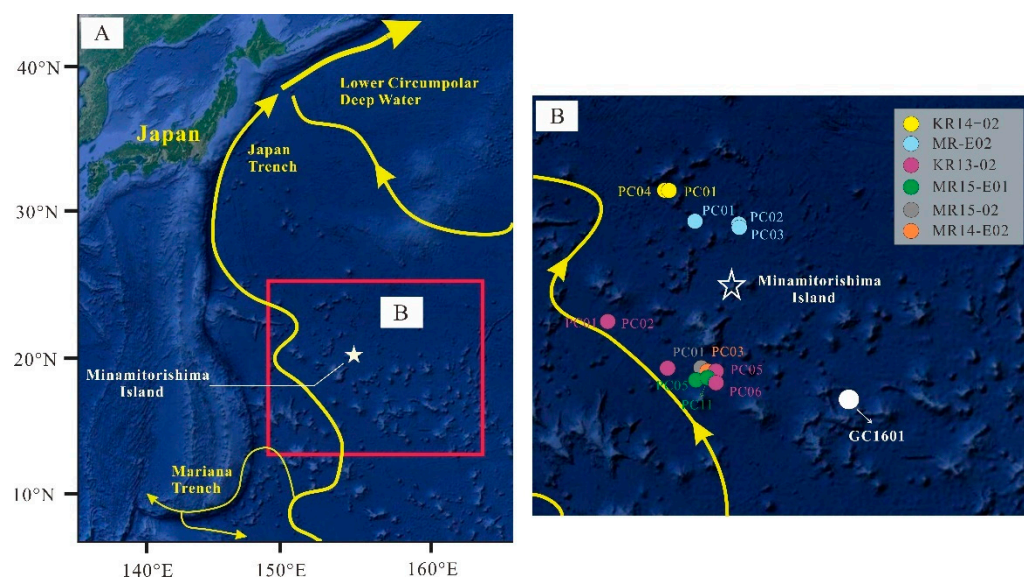

Figure 9. Locations of the Northwest Pacific and GC1601 core (Base map according to Google Earth). (**A**) Location of Northwest Pacific, the yellow lines represent Lower Circumpolar Deep Water (LCDW) in this area [68,69], the red highlighted by the red rectangle in (**A**) is shown in (**B**). (**B**) Locations of GC1601 and other sediments cores in the Sea area of Minamitorishima Island, these colored sediments cores are from [7,10].

In contrast, the sediments in the East and the North Sea area of Minamitorishima Island were relatively weakly influenced by LCDW (Figure 9); besides, material sources of these two areas are also dominated by terrigenous materials, which makes them very difficult to form REY-rich muds.

6. Conclusions

(1) M/I (montmorillonite/illite) and the Sr-Nd isotopic characteristics indicate that the sediments in the study area are dominated by terrestrial materials. Considering that the study area is far away from the mainland and in the downwind direction of the East Asian monsoon, it is speculated that the terrigenous components of the sediments in the study area are likely to be East Asian dust.

(2) The εNd of GC1601 is positively correlated with P_2O_5, Co, Ni, and Cu, and approaching εNd of seawater with increasing depth, indicating that the sedimentary environment in the area is relatively stable.

(3) Most of the sediments in the study area are not highly enriched in REY due to the larger supply of dust materials. By contrast, sediments in the South Sea area of Minamitorishima Island may be influenced by the strong bottom current, which makes their sediment rate relatively low with considerable enriched REY contents.

Author Contributions: Conceptualization, W.M., C.T. and Z.Q.; methodology, Z.Q.; software, Z.Q.; validation, W.M. and C.T.; formal analysis, Z.Q.; investigation, W.M., C.T. and Z.Q.; resources, W.M. and C.T.; data curation, Z.Q. and W.M.; writing—original draft preparation, Z.Q.; writing—review and editing, all authors; visualization, W.M., C.T., A.K. and S.H.; supervision, W.M. and C.T.; project administration, W.M. and C.T.; funding acquisition, W.M., C.T. and S.H. All authors have read and agreed to the published version of the manuscript.

Conflicts of Interest: The authors declare no conflict of interest.

References

1. Shepard, F.P.; Moore, D.G. Post-glacial stratigraphy alog the central Texas coast. *J. Sediment. Res.* **1954**, *24*, 140. [CrossRef]
2. Qiu, Z.; Ma, W.; Zhang, X.; Ren, J. Geochemical characteristics of sediments in the southeastern waters of Nanjiao Island and their significance in indicating rare earth resources. *Geol. Sci. Technol. Inf.* **2019**, *38*, 205–214. (In Chinese)
3. Okamoto, N.; Usui, A. Regional Distribution of Co-Rich Ferromanganese Crusts and Evolution of the Seamounts in the Northwestern Pacific. *Mar. Georesources Geotechnol.* **2014**, *32*, 187–206. [CrossRef]
4. Qiu, Z.; Dong, Y.; Ma, W.; Zhang, W.; Yang, K.; Zhao, H. Geochemical characteristics of platinum-group elements in polymetallic nodules from the Northwest Pacific Ocean. Acta Oceanological Sinica. *Acta Oceanol. Sin.* **2020**, *39*, 34–42. [CrossRef]
5. Qiu, Z.; Ma, W.; Yang, K. Characteristics of platinum group elements in submarine polymetallic nodules and their resource implications. *J. Zhejiang Univ. (Sci. Ed.)* **2021**, *48*, 221–230. (In Chinese)
6. Yasukawa, K.; Kino, S.; Ohta, J.; Azami, K.; Tanaka, E.; Mimura, K.; Fujinaga, K.; Nakamura, K.; Kato, Y. Stratigraphic Variations of Fe–Mn Micronodules and Implications for the Formation of Extremely REY-rich Mud in the Western North Pacific Ocean. *Minerals* **2021**, *11*, 270. [CrossRef]
7. Fujinaga, K.; Yasukawa, K.; Nakamura, K.; Machida, S.; Takaya, Y.; Ohta, J.; Araki, S.; Liu, H.; Usami, R.; Maki, R.; et al. Geochemistry of REY-rich mud in the Japanese Exclusive Economic Zone around Minamitorishima Island. *Geochem. J.* **2016**, *50*, 575–590. [CrossRef]
8. Qiu, Z.; Ma, W.; Zhang, X.; Dong, Y.; Zhang, W.; Yang, K. Geochemical characteristics of surface sediments in the Northwest Pacific Ocean and their source-indicating significance. *J. Zhejiang Univ. (Sci. Ed.)* **2020**, *47*, 1–10. (In Chinese)
9. Qiu, Z.; Ma, W. REY Resource Potential of Sediments in Sea Area of Minamitorishima Island: Evidence from REY Geochemistry of 21 Box Cores. *Acta Geol. Sin. (Engl. Ed.)* **2019**, *93* (Suppl. S2), 117.
10. Takaya, Y.; Yasukawa, K.; Kawasaki, T.; Fujinaga, K.; Ohta, J.; Usui, Y.; Nakamura, K.; Kimura, J.I.; Chang, Q.; Hamada, M.; et al. The tremendous potential of deep-sea mud as a source of rare-earth elements. *Sci. Rep.* **2018**, *8*, 5763. [CrossRef]
11. Hein, J.R.; Conrad, T.A.; Dunham, R.E. Seamount Characteristics and Mine-Site Model Applied to Exploration- and Mining-Lease-Block Selection for Cobalt-Rich Ferromanganese Crusts. *Mar. Georesources Geotechnol.* **2009**, *27*, 160–176. [CrossRef]
12. Hein, J.R.; Conrad, T.A.; Staudigel, H. Seamount Mineral Deposits: A Source of Rare Metals for High-Technology Industries. *Oceanography* **2010**, *23*, 184–189. [CrossRef]
13. Hein, J.R.; Mizell, K.; Koschinsky, A.; Tracey, A.; Conrad, A. Deep-ocean mineral deposits as a source of critical metals for high- and green-technology applications: Comparison with land-based resources. *Ore Geol. Rev.* **2013**, *51*, 1–14. [CrossRef]
14. Nishi, K.; Usui, A.; Nakasato, Y.; Yasuda, H. Formation age of the dual structure and environmental change recorded in hydrogenetic ferromanganese crusts from Northwest and Central Pacific seamounts. *Ore Geol. Rev.* **2017**, *87*, 62–70. [CrossRef]

15. Usui, A.; Nishi, K.; Sato, H.; Nakasato, Y.; Thornton, B.; Kashiwabara, T.; Tokumaru, A.; Sakaguchi, A.; Yamaoka, K.; Kato, S. Continuous growth of hydrogenetic ferromanganese crusts since 17Myr ago on Takuyo-Daigo Seamount, NW Pacific, at water depths of 800–5500 m. *Ore Geol. Rev.* **2017**, *87*, 71–87. [CrossRef]

16. Frey, F.A.; Coffin, M.F.; Wallace, P.J.; Teagle, D.A.H. Leg 183 synthesis: Kerguelen Plateau–Broken Ridge—A large igneous province. In *Proceedings of the Ocean Drilling Program, Scientific Results*; Texas A & M University Ocean Drilling Program: College Station, TX, USA, 2003; Volume 183. Available online: https://eprints.soton.ac.uk/50788/ (accessed on 13 December 2021).

17. Scudder, R.P.; Murray, R.W.; Plank, T. Dispersed ash in deeply buried sediment from the northwest Pacific Ocean: An example from the Izu-Bonin arc (ODP Site 1149). *Earth Planet. Sci. Lett.* **2009**, *284*, 639–648. [CrossRef]

18. Alt, J.C.; Teagle, D. Hydrothermal alteration of upper oceanic crust formed at a fast-spreading ridge: Mineral, chemical, and isotopic evidence from ODP Site. *Chem. Geol.* **2003**, *201*, 191–211. [CrossRef]

19. Rouxel, O.; Dobbek, N.; Ludden, J.; Fouquet, Y. Iron isotope fractionation during oceanic crust alteration. *Chem. Geol.* **2003**, *202*, 155–182. [CrossRef]

20. Biscaye, E. Mineralogy and sedimentation of recent deep-sea clay in atlantic ocean and adjacent areas and oceans. *Bull. Geol. Soc. Am.* **1965**, *76*, 803–832. [CrossRef]

21. Chen, W.; Zhu, G.; Zhang, K.; Zhang, Y.; Yan, H.; Du, D.; Zhang, Z.; Xia, B. Late Neoproterozoic intracontinental rifting of the Tarim carton, NW China: An integrated geochemical, geochronological and Sr-Nd-Hf isotopic study of siliciclastic rocks and basalts from deep drilling cores. *Gondwana Res.* **2020**, *80*, 142–156. [CrossRef]

22. Sattarova, V.V.; Artemova, A.V. Geochemical and micropaleontological character of Deep-Sea sediments from the Northwestern Pacific near the Kuril–Kamchatka Trench. *Deep. Sea Res. Part II Top. Stud. Oceanogr.* **2015**, *111*, 10–18. [CrossRef]

23. Ming, J.; Li, C.; Huang, J.; Shi, M. Assemblage characteristics of clay minerals and its implications to evolution of eolian dust input to the Parece Vela Basin since 1.95 Ma. *Chin. J. Oceanol. Limnol.* **2014**, *32*, 174–186. [CrossRef]

24. Kong, X.; Xiang, G. A discussion on the study of clay minerals from ocean sediments and global change. *Trans. Oceanol. Limnol.* **2003**, *1*, 22–26. (In Chinese)

25. Khan, M.; Liu, J.; Liu, S.; Seddique, A.; Cao, L.; Rahman, A. Clay mineral compositions in surface sediments of the Ganges-Brahmaputra-Meghna River system of Bengal Basin, Bangladesh. *Mar. Geol.* **2019**, *412*, 27–36. [CrossRef]

26. Nayak, K.; Lin, T.S.; Huang, K.F.; Liu, Z.; Hsu, S. Clay-mineral distribution in recent deep-sea sediments around Taiwan: Implications for sediment dispersal processes. *Tectonophysics* **2021**, *814*, 228974. [CrossRef]

27. Charpentier, D.; Buatier, M.D.; Jacquot, E.; Gaudin, A.; Wheat, C.G. Conditions and mechanism for the formation of iron-rich Montmorillonite in deep sea sediments (Costa Rica margin): Coupling high resolution mineralogical characterization and geochemical modeling. *Geochim. Cosmochim. Acta* **2011**, *75*, 1397–1410. [CrossRef]

28. Cole, T.G.; Shaw, H.F. The nature and origin of authigenic smectites in some Recent marine sediments. *Clay Miner.* **1983**, *18*, 239–252. [CrossRef]

29. Singer, A.; Stoffers, P.; Heller-Kallai, L.; Szafranek, D. Nontronite in a deep-sea core from the South Pacific. *Clays Clay Miner.* **1984**, *32*, 375–383. [CrossRef]

30. Wan, S.; Yu, Z.; Clift, P.D.; Sun, H.; Li, T. History of Asian eolian input to the West Philippine Sea over the last one million years. *Paleogeography Palaeoclimatol. Paleoecol.* **2012**, *326*, 152–159. [CrossRef]

31. Fu, F.; Yao, X.; Ni, J. Mineral and geochemical characteristics of surface sediment clays in the western part of the eastern Pacific CC area. *Oceanogr. Res.* **2017**, *35*, 55–65. (In Chinese)

32. Kohler, B.; Singer, A.; Stoffers, P. Biogenic nontronite from marine white smoker chimneys. *Clays Clay Miner.* **1994**, *42*, 689–701. [CrossRef]

33. Corliss, J.B.; Lyle, M.; Dymond, J. The chemistry of hydrothermal mounds near the Galapagos Rift. *Earth Planet. Sci. Lett.* **1978**, *40*, 12–24. [CrossRef]

34. Chamley, H. *Clay Formation Through Weathering*; Springer: Berlin/Heidelberg, Germany, 1989.

35. Fang, D.J.; Yang, Z.S.; Mao, D.; Guo, Z. Composition of clay minerals and geochemical components in Yangtze and Yellow River sediments. *Mar. Geol. Quat. Geol.* **2001**, *21*, 7–12. (In Chinese)

36. Wang, F.; He, G.; Wang, H.; Ren, J. Rare earth geochemical characteristics of columnar sediments in the Mariana Trench and their indicative significance. *Mar. Geol. Quat. Geol.* **2016**, *36*, 67–75. (In Chinese)

37. Shi, Y.; Xu, D.; Li, J.; Wang, J. Clay minerals in the Late Interglacial Lanzhou Loess Record and their environmental significance. *Mar. Geol. Quat. Geol.* **1997**, *17*, 87–94. (In Chinese)

38. Ren, M.; Shi, Y. Sediment discharge of the Yellow River (China) and its effect on the sedimentation of the Bohai and the Yellow Sea. *Cont. Shelf Res.* **1986**, *6*, 785–810. [CrossRef]

39. Yang, S.Y.; Jung, H.S.; Choi, M.S.; Li, C.X. The rare earth element compositions of the Changjiang (Yangtze) and Huanghe (Yellow) river sediments. *Earth Planet. Sci. Lett.* **2002**, *201*, 407–419. [CrossRef]

40. Yang, S.Y.; Jung, H.S.; Lim, D.I.; Li, C.X. A review on the provenance discrimination of sediments in the Yellow Sea. *Earth-Sci. Rev.* **2003**, *63*, 93–120. [CrossRef]

41. Wan, S.; Li, A.; Clift, P.D.; Stuut, J.W. Development of the East Asian monsoon: Mineralogical and sedimentologic records in the northern South China Sea since 20 Ma. *Paleogeography Palaeoclimatol. Paleoecol.* **2007**, *254*, 561–582. [CrossRef]

42. Zhang, D.Y. Composition and distribution characteristics of clay minerals in the Mariana Trough. *J. Oceanogr. Huanghai Bohai Seas* **1994**, *12*, 32–39. (In Chinese)

43. Chi, Y.; Li, A.; Jiang, F.; Wan, S. Characterization of clay mineral assemblages and physical source analysis in the eastern Luzon Sea. *Mar. Sci.* **2009**, *33*, 80–88. (In Chinese)

44. Shi, X.F.; Wang, Z.L. Genetic mineralogy of clay sediments in the western Philippine Sea. *Mar. Geol. Quat. Geol.* **1995**, *15*, 61–72. (In Chinese)

45. Liu, J. *Geochemical Characteristics of Rare Earth Elements and Nd Isotopes in East Pacific Sediments and Their Environmental Indications*; Graduate School of Chinese Academy of Sciences (Institute of Oceanography): Beijing, China, 2004. (In Chinese)

46. Chen, J.; Li, G.; Yang, J.; Rao, W.; Lu, H.; Balsam, W.; Sun, Y.; Ji, J. Nd and Sr isotopic characteristics of Chinese deserts: Implications for the provenances of Asian dust. *Geochim. Cosmochim. Acta* **2007**, *71*, 3904–3914. [CrossRef]

47. Liu, E.; Wang, X.; Zhao, J.; Wan, J. Geochemical and Sr-Nd isotopic variations in a deep-sea sediment core from Eastern Indian Ocean: Constraints on dust provenances, paleoclimate and volcanic eruption history in the last 300,000 years. *Mar. Geol.* **2015**, *367*, 38–49. [CrossRef]

48. Kessarkar, P.M.; Rao, V.P.; Ahmad, S.M.; Babu, G.A. Clay minerals and Sr–Nd isotopes of the sediments along the western margin of India and their implication for sediment provenance. *Mar. Geol.* **2003**, *202*, 55–69. [CrossRef]

49. Yang, J.; Li, G.; Rao, W.; Ji, J. Isotopic evidences for provenance of East Asian Dust. *Atmos. Environ.* **2009**, *43*, 4481–4490. [CrossRef]

50. Wu, W.; Xu, S.; Yang, J.; Yin, H.; Lu, H.; Zhang, K. Isotopic characteristics of river sediments on the Tibetan Plateau. *Chem. Geol.* **2010**, *269*, 406–413. [CrossRef]

51. Shao, L.; Li, C.A.; Zhang, Y.F.; Yuan, S.; Wang, J.; Jiang, H.; Zhao, J. Strontium-Nd isotopic composition and source tracing of sediments in the upper Yangtze River system. *J. Sedimentol.* **2014**, *32*, 290–295. (In Chinese)

52. Han, Z.; Liu, H.; Li, M.; Sun, X.; Lai, Z.; Bian, Y.; Lin, X. Characterization of basaltic rock geochemistry and mantle source regions in the near-equatorial region of the East Pacific Rise. *J. Ocean. Univ. China (Nat. Sci. Ed.)* **2018**, *48*, 63–75. (In Chinese)

53. Guo, P.; Niu, Y.; Sun, P.; Zhang, J.; Chen, S.; Duan, M.; Gong, H.; Wang, X. The nature and origin of upper mantle heterogeneity beneath the Mid-Atlantic Ridge 33–35° N: A Sr-Nd-Hf isotopic perspective. *Geochim. Cosmochim. Acta* **2021**, *307*, 72–85. [CrossRef]

54. Luo, W.Q. *Influence of Subduction Components on Magmatism in the Back-Arc Basin*; Ocean University of China: Qingdao, China, 2007. (In Chinese)

55. Pettke, T.; Halliday, A.N.; Hall, C.M.; Rea, D. Dust production and deposition in Asia and the north Pacific Ocean over the past 12 Myr. *Earth Planet. Sci. Lett.* **2000**, *178*, 397–413. [CrossRef]

56. Ding, Z.L.; Sun, J.M.; Yang, S.L.; Liu, T.S. Geochemistry of the Pliocene red clay formation in the Chinese Loess Plateau and implications for its origin, source provenance and paleoclimate change. *Geochim. Cosmochim. Acta* **2001**, *65*, 901–913. [CrossRef]

57. Kanayama, S.; Yabuki, S.; Yanagisawa, F.; Motoyama, R. The chemical and strontium isotope composition of atmospheric aerosols over Japan: The contribution of long-range-transported Asian dust (Kosa). *Atmos. Environ.* **2002**, *36*, 5159–5175. [CrossRef]

58. Mori, I.; Nishikawa, M.; Quan, H.; Morita, M. Estimation of the concentration and chemical composition of kosa aerosols at their origin. *Atmos. Environ.* **2002**, *36*, 4569–4575. [CrossRef]

59. Yasukawa, K.; Ohta, J.; Miyazaki, T.; Vaglarov, B.; Chang, Q.; Ueki, K.; Toyama, C.; Kimura, J.; Tanaka, E. Nakamura, K. Statistic and Isotopic Characterization of Deep-Sea Sediments in the Western North Pacific Ocean: Implications for Genesis of the Sediment Extremely Enriched in Rare Earth Elements. *Geochem. Geophys. Geosystems* **2019**, *20*, 3402–3430. [CrossRef]

60. Feng, X.G. *Response of Wind and Dust Input to East Asian Paleoclimate in the Amami Delta Basin Since the Quaternary*; University of Chinese Academy of Sciences (Institute of Oceanography, Chinese Academy of Sciences): Beijing, China, 2019. (In Chinese)

61. Wang, F.; He, G.; Lai, P. Nd isotope characteristics and physical significance of Pacific rare earth-rich deep-sea sediments and clay fractions (<2 μm). *Geotecton. Metallog.* **2019**, *43*, 292–302. (In Chinese)

62. Amakawa, H.; Nozaki, Y.; Alibo, D.S.; Zhang, J.; Fukugawa, K.; Nagai, H. Neodymium isotopic variations in Northwest Pacific waters. *Geochim. Cosmochim. Acta* **2004**, *68*, 715–727. [CrossRef]

63. Yasukawa, K.; Liu, H.; Fujinaga, K.; Machida, S.; Haraguchi, S.; Ishii, T.; Nakamura, K.; Kato, Y. Geochemistry and mineralogy of REY-rich mud in the eastern Indian Ocean. *J. Asian Earth Sci.* **2014**, *93*, 25–36. [CrossRef]

64. Iijima, K.; Yasukawa, K.; Fujinaga, K.; Machida, S.; Haraguchi, S.; Ishii, T.; Nakamura, K.; Kato, Y. Discovery of extremely REY-rich mud in the western North Pacific Ocean. *Geochem. J.* **2016**, *50*, 557–573. [CrossRef]

65. Sun, X.; Sa, R.; He, G.; Xu, L.; Pan, Q.; Liao, J.; Zhu, K.; Deng, X. Enrichment of rare earth elements in siliceous sediments under slow deposition: A case study of the central North Pacific. *Ore Geol. Rev.* **2018**, *94*, 12–32.

66. Yasukawa, K.; Nakamura, K.; Fujinaga, K.; Iwamori, H.; Kato, Y. Tracking the spatiotemporal variations of statistically independent components involving enrichment of rare-earth elements in deep-sea sediments. *Sci. Rep.* **2016**, *6*, 29603. [CrossRef]

67. Yasukawa, K.; Nakamura, K.; Fujinaga, K.; Machida, S.; Kato, Y. Rare-earth, major, and trace element geochemistry of deep-sea sediments in the Indian Ocean: Implications for the potential distribution of REY-rich mud in the Indian Ocean. *Geochem. J.* **2015**, *49*, 621–635. [CrossRef]

68. Behrens, K.; Katharina, P.; Bernhard, S.; Brumsack, H. Sources and processes affecting the distribution of dissolved Nd isotopes and concentrations in the West Pacific. *Geochim. Cosmochim. Acta* **2018**, *222*, 508–534. [CrossRef]

69. Kawabe, M.; Fujio, S. Pacific Ocean circulation based on observation. *J. Oceanogr.* **2010**, *66*, 389–403. [CrossRef]